INFECTION AND IMMUNITY, Oct. 1995, p. 3936–3944 Vol. 63, No. 10
0019-9567/95/$04.00+0

Escherichia coli Cytotoxic Necrotizing Factor 1: Evidence for Induction of Actin Assembly by Constitutive Activation of the p21 Rho GTPase

CARLA FIORENTINI,[1]* GIANFRANCO DONELLI,[1] PAOLA MATARRESE,[1] ALESSIA FABBRI,[1] SILVIA PARADISI,[1] AND PATRICE BOQUET[2]

Department of Ultrastructures, Istituto Superiore di Sanità, 00161 Rome, Italy,[1] and Unitè des Toxines Microbiennes, Institut Pasteur, Paris Cedex 15, France[2]

Received 7 April 1995/Returned for modification 14 June 1995/Accepted 18 July 1995

Cytotoxic necrotizing factor type 1 (CNF1) induces in HEp-2 cells an increase in F-actin structures, which was detectable by fluorescence-activated cell sorter analysis 24 h after addition of this factor to the culture medium. Increase in F-actin was correlated with the augmentation of both the cell volume and the total cell actin content. Actin assembly-disassembly is controlled by small GTP-binding proteins of the Rho family, which have been reported recently to be modified by CNF1 treatment. *Clostridium difficile* toxin B and *Clostridium botulinum* exoenzyme C3, both known to act on the Rho GTPase, were used as biological tools to study the effect of CNF1 on this protein. CNF1 incubated before, during, or after exposure to the chimeric toxin C3B (which is the product of a genetic fusion between the DNA coding for C3 and the one coding for the B fragment of diphtheria toxin) protected HEp-2 cells from the disruption of F-actin structures caused by inactivation of the Rho GTPase through its ADP-ribosylation. On the other hand, *C. difficile* toxin B cytopathic effect was not observed upon preincubation of cells with CNF1. Toxins acting through a Rho-independent mechanism, such as cytochalasin D and *Clostridium spiroforme* iota-like toxin, could not be modified in their cellular activities by CNF1 treatment. All of our results suggest that CNF1 modifies the Rho molecule, thus probably protecting this GTPase from further bacterial toxin modification.

Certain *Escherichia coli* strains of clinical relevance have been reported to elaborate a toxin-like protein named cytotoxic necrotizing factor 1 (CNF1) (7). CNF1 is a monomeric protein with a molecular mass of 110 kDa which causes necrosis in rabbit skin upon injection and multinucleation in cultured cells. Most CNF1-producing strains of *E. coli* are hemolytic, and the genes encoding CNF1, alpha-hemolysin, and a cell adhesion pyelonephritogenic adherence pilus (PAP) factor are located in close proximity on the bacterial chromosome (12). The CNF1 nucleotide gene has been reported recently, and part of it showed a striking homology with the mitogenic toxin from *Pasteurella multocida* (13).

CNF1 production was first observed in *E. coli* strains isolated from humans with diarrhea (7). Subsequently, CNF1-producing strains were frequently isolated from *E. coli* causing urinary tract infections (8). Bacterial blood isolates, from patients with bacteremia caused by *E. coli* infections, have often been found to contain CNF1-producing bacteria (5). The spreading of such intestinal *E. coli* organisms from the lumenal side of the gut (or the urinary tract) to the bloodstream might be explained by the potent phagocyte-like activity that CNF1 induces in cells (15).

Bacterial entry into cells is a process which requires G-actin assembly into F-actin since it can be blocked by cytochalasin D (CD) (14, 18). Very interestingly, CNF1 has been described as interacting with the actin cytoskeleton, promoting cell spreading and probably interfering with cytokinesis (16). The main effect of CNF1 on the actin cytoskeleton is a time- and dose-dependent increase in stress fibers and membrane ruffling (15). It is now clear that F-actin cytoskeleton assembly-disassembly is controlled by proteins belonging to the Ras-like p21 Rho family (19). In mammalian cells, the Rho family consists of the Rac, Rho, G25K, and CDC42 subfamilies (19). The Rac subfamily consists of two members, Rac1 and Rac2, and regulates not only membrane ruffling in Swiss 3T3 cells (28) but also NADPH oxidase-catalyzed superoxide formation in neutrophils (1). The Rho subfamily, which comprises the three highly related proteins RhoA, RhoB, and RhoC, has been described as controlling the assembly of focal adhesions and actin stress fibers in response to growth factors in Swiss 3T3 cells (27). Only this subfamily is ADP-ribosylated by *Clostridium botulinum* ADP-ribosyltransferase C3 (2, 9). Like all proteins belonging to the Ras-related small G-protein superfamily, the mammalian Rho proteins become activated upon GTP binding and have intrinsic GTPase activity that hydrolyzes the bound GTP, rendering the proteins inactive. We have recently shown that upon incubation of cells with CNF1, the Rho GTPase was shifted to a higher molecular weight compared with that of control untreated cells (17, 23). This indicates a possible direct modification of the Rho protein by CNF1 which results in GTPase activation. Interestingly, CNF1-treated cells exhibit a phenotype similar to the one observed in cells after microinjection of constitutively activated Rho GTPase (24).

In this work, using toxins acting specifically on the Rho GTPase, we found evidence supporting the idea that upon entry into the cell cytosol, CNF1 modifies this GTP-binding molecule to constitutively activate it.

MATERIALS AND METHODS

Cell cultures. HEp-2 cells were grown at 37°C in Dulbecco modified Eagle medium (DMEM), supplemented with 5% fetal calf serum (Flow Laboratories, Irvine, United Kingdom), 1% nonessential amino acids, 5 mM L-glutamine, penicillin (100 U/ml), and streptomycin (100 μg/ml). The subcultures were serially propagated after harvesting with 10 mM EDTA and 0.25% trypsin in phosphate-buffered saline (PBS; pH 7.4).

Toxins. CNF1 was purified as described previously (11) from the *E. coli* BM2-1

* Corresponding author. Mailing address: Department of Ultrastructures, Istituto Superiore di Sanità, Viale Regina Elena 299, 00161 Rome, Italy. Phone: 6-49902905. Fax: 6-4957634.

strain. *Clostridium difficile* toxin B (CdB) was a kind gift from Cristoph von Eichel-Streiber of Mainz University (Mainz, Germany). The C3B chimeric toxin was produced and purified as described by Aullo and coworkers (4). Pure diphtheria toxin (DT) was produced and purified in our laboratory. Purification of iota-like toxin components I and II from cultures of *Clostridium spiroforme* (strain NCTC 11493; Rhone-Mérieux collection no. 15991) was achieved as reported previously (26).

Cell treatments. Forty-eight hours after seeding on glass coverslips in 24-well plates (initial inoculum, 10^4 cells per ml), HEp-2 cells were treated with toxins. For each toxin, the following concentrations have been used: 10^{-10} M for CNF1, 10^{-9} M for C3B, 10^{-12} M for CdB, 10^{-9} M for *C. spiroforme* iota-like toxin, and 2 μg/ml for CD. Experiments were performed as indicated in Results. After treatment, cultures were prepared for fluorescence microscopy, scanning electron microscopy, and flow cytometry. All of the experiments were performed at least three times, with triplicate samples for each point.

Flow cytometry. Treated and control HEp-2 cells were pelleted, fixed in 70% ice-cold methanol, and washed twice in PBS. For F-actin detection, cells were stained with fluorescein isothiocyanate (FITC)-phalloidin (Sigma) at a final concentration of 0.1 mg/ml for 30 min at 37°C, whereas for the analysis of G-actin, DNase I-FITC, a protein capable of binding monomeric actin, was used at a concentration of 83 μg/ml for 30 min at 37°C. For total actin labeling, anti-actin monoclonal antibodies (Chemicon) were incubated with cells for 30 min at 37°C, and then for a further 30 min with FITC–anti-mouse immunoglobulin G F(ab′)$_2$ fragment (Boehringer Mannheim). Fluorescence measurements were made with a FACScan flow cytometer (Becton Dickinson) equipped with a 488-nm argon ion laser, and green fluorescence was collected by use of a 530/30-nm band pass filter. Data were recorded and analyzed with a Hewlett-Packard computer with Lysis II software (Becton Dickinson).

Volume analysis. The HEp-2 cell volume was analyzed after 1, 3, 6, 12, 24, and 48 h of treatment with 10^{-10} M CNF1. Control and treated cells, harvested with 10 mM EDTA and 0.25% trypsin in PBS, were resuspended in DMEM and then diluted 1:20 in an isotonic solution. Cell volume was assessed with a Coulter Counter ZM11. Student's *t* test was used.

Fluorescence microscopy. HEp-2 cells were grown on 13-mm-diameter glass coverslips in separate wells (5×10^4 cells per well) in a 37°C incubator containing an atmosphere of 95% air–5% CO_2. Following toxin treatments, both control and treated cells were fixed with 3.7% formaldehyde in PBS with 2% bovine serum albumin for 10 min at room temperature. After washing in the same buffer, the cells were permeabilized with 0.5% Triton X-100 (Sigma Chemical Co., St. Louis, Mo.) in PBS for 10 min at room temperature. For F-actin detection, cells were stained with fluorescein-phalloidin (Sigma; working dilution, 1:500) at 37°C for 30 min. For fimbrin detection, polyclonal antibodies directed against fimbrin (a kind gift from Monique Arpin, Institut Pasteur, Paris, France; working dilution, 1:200) were used. Following incubation for 30 min at 37°C, cells were washed and then incubated with a sheep anti-rabbit immunoglobulin M fluorescein-linked whole antibody (Sigma) for 30 min at 37°C. Finally, after washing, coverslips were mounted with glycerol-PBS (2:1) and analyzed with a Nikon Microphot fluorescence microscope.

Scanning electron microscopy. Control and treated cells were fixed with 2.5% glutaraldehyde in 0.1 M cacodylate buffer (pH 7.4) at room temperature for 20 min. Following postfixation in 1% OsO_4 for 30 min, cells were dehydrated through graded ethanols, critical point dried in CO_2, and gold coated by sputtering. The samples were examined with a Cambridge 360 scanning electron microscope.

Inhibition of cell protein synthesis by DT. HEp-2 cells were incubated for 48 h in medium with or without 10^{-10} M CNF1. Cells were then treated with various doses of DT (10^{-8} to 10^{-12} M) for 18 h. The medium was then removed and replaced with DMEM without L-leucine but containing 0.02 mCi of [^{14}C]leucine, and the incubation was prolonged for 1 h. Cell monolayers were then precipitated by 10% trichloroacetic acid and washed three times with 5% trichloroacetic acid, and after solubilization with NaOH, the radioactivity incorporated into proteins was evaluated by liquid scintillation counting. Protein synthesis is expressed as the percentage of total protein synthesis of control cells not treated with DT.

RESULTS

CNF1 increases the amount of F-actin in HEp-2 cells. As reported previously (15, 16), the most evident morphological change caused by CNF1 in cultured cells is the increase of structure rich in F-actin. To evaluate quantitatively the F-actin assembly, flow cytometry was used to analyze cells treated with CNF1 for 1, 3, 6, 12, 24, and 48 hours. In Fig. 1a to c, fluorescence histograms of cells (control cells and cells exposed to CNF1 for 12, 24, and 48 h) stained with FITC-phalloidin (which labels F-actin) are shown. Differences between control and treated cells became significant after 24 h of CNF1 treatment, and expression of F-actin increased from 24 to 48 h. In Fig. 1d to f, fluorescence histograms of cells labelled with DNase I-FITC (which detects actin monomers) demonstrated that no difference was detectable after CNF1 treatment whatever the incubation time of cells with CNF1. Starting from 24 to 48 h, treatment with CNF1 thus induced a clear, detectable increase in polymerized actin without any decrease in cell monomeric actin content. Total actin content (G-actin plus F-actin) upon detection with an anti-actin antibody which reacts with both G-actin and F-actin clearly increased after 24 and 48 h of exposure to CNF1 (Fig. 1g to i). Volume histograms of control and CNF1-treated cells, obtained with a Coulter Counter (Fig. 1l to n), showed that CNF1 was able to significantly increase the cell volume after 24 and 48 h.

CNF1 overcomes the inactivation of Rho by *C. botulinum* exoenzyme C3. ADP-ribosylation of Rho, induced by *C. botulinum* exoenzyme C3, provokes a loss of actin filaments (9). However, exoenzyme C3 by itself cannot enter cells since it has no cell binding and membrane translocation domains like the B chain of DT. To overcome this problem, we used a chimeric toxin which is the product of a genetic fusion between the DNA coding for exoenzyme C3 and the one coding for the B fragment of DT (4). The B fragment of DT linked to C3 allows the penetration of the exoenzyme in the cytosol, as long as the target cells possess DT receptors. Since HEp-2 cells are sensitive to DT, the chimeric C3B toxin was used in these cells to modulate the Rho protein in vivo before, during, and after treatment with CNF1. We checked first whether HEp-2 cells treated with CNF1 were still sensitive to DT, to rule out the possibility that CNF1 could have altered the entry mechanism of DT. We did find that CNF1-treated HEp-2 cells were indeed sensitive to DT (data not shown).

As observed by scanning electron microscopy (Fig. 2A), control cells were polygonal, with numerous thin microvilli studding the cell surface (Fig. 2Aa). After treatment with CNF1 for 48 h, the cells appeared to be spread on the substrate and flattened, with evident ruffles on both the surface and the cell periphery (Fig. 2Ab). The evident cell retraction caused by exposure to C3B for 36 h (Fig. 2Ac) was prevented by the simultaneous addition of CNF1 (Fig. 2Ad). In the latter case, the cell phenotype was nearly identical to the one shown by cells treated with CNF1 alone. Fluorescence microscopy observations (Fig. 2B) showed modifications in actin microfilament organization upon treatment with CNF1. Control HEp-2 cells were characterized by a poorly developed actin network (Fig. 2Ba), whereas exposure to CNF1 induced a thickening of stress fibers and formation of large ruffles (Fig. 2Bb). Complete disorganization of the actin network was observed after 36 h of treatment with C3B (Fig. 2Bc). Simultaneous exposure of HEp-2 cells to C3B and CNF1 prevented the modification of F-actin structures induced by C3B, microfilaments being organized as they are in CNF1-treated cells (Fig. 2Bd). The distribution pattern of the actin-binding and -bundling protein fimbrin (6) showed differences between CNF1-treated cells and control cells (Fig. 2C). In untreated HEp-2 cells, fimbrin did not colocalize with defined structures but was distributed either as patches or as filaments (Fig. 2Ca). By contrast, in CNF1-treated cells, fimbrin was observed to be closely associated with the leading edges of the ruffling membranes (Fig. 2Cb). Complete disappearance of fluorescent staining of fimbrin was observed after C3B exposure (Fig. 2Cc). Incubation of cells with CNF1 in association with C3B gave rise to a fimbrin-staining pattern similar to the one observed in CNF1-treated cells (Fig. 2Cd).

When CNF1 was added to cells treated with C3B for 36 h, it was still able to overcome the cell body retraction induced by C3B (Fig. 3). This effect was already visible after a CNF1 treatment as short as 6 h (Fig. 3a and b). Exposure to CNF1 for

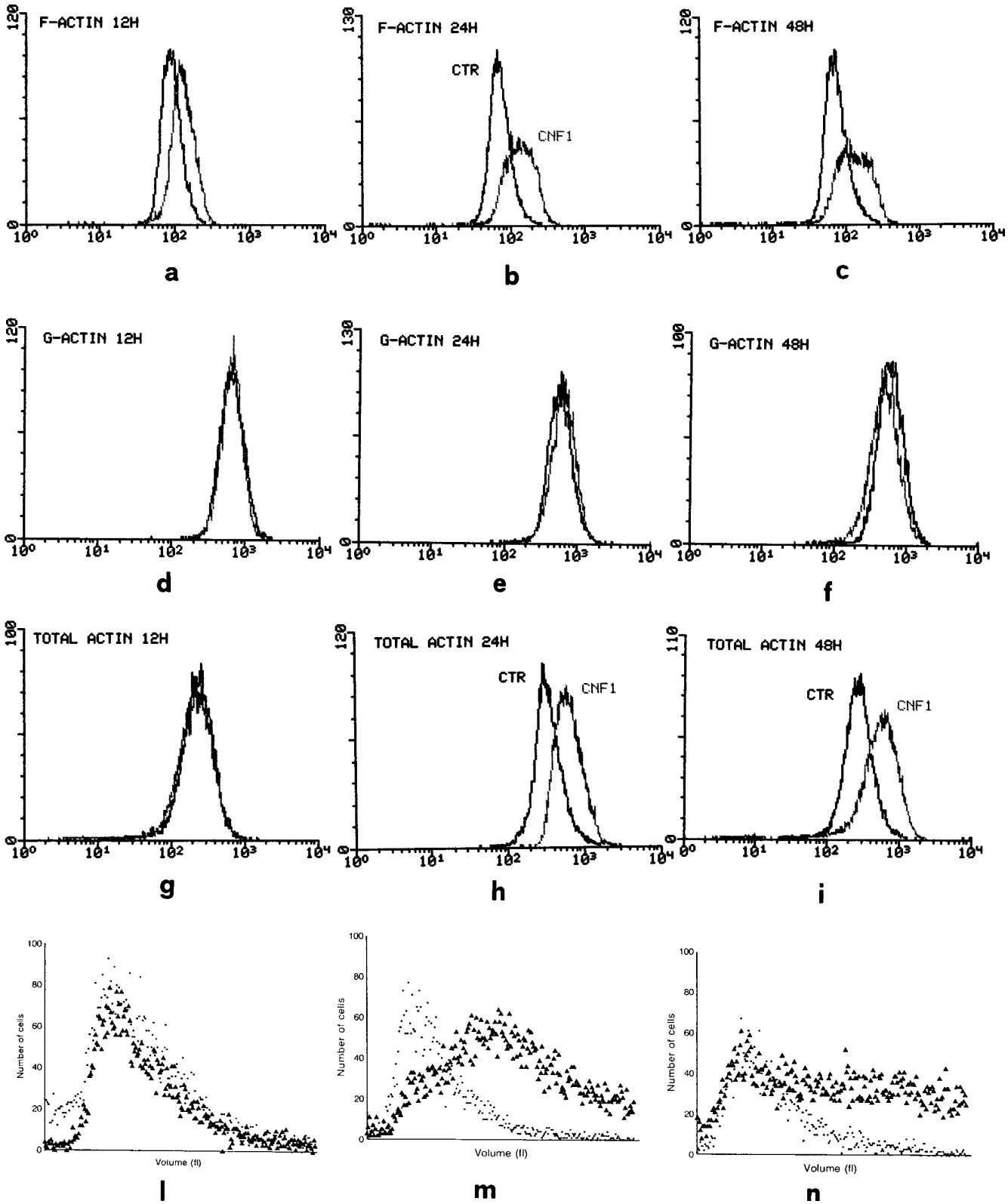

FIG. 1. CNF1 increases the amount of F-actin in HEp-2 cells. HEp-2 cells were exposed to CNF1 for 12, 24, and 48 h (left, middle, and right panels, respectively. (a to c) Fluorescence histograms of overlying control (black line) and CNF1-treated (gray line) cells stained with FITC-phalloidin for F-actin detection. The histograms of treated cells were shifted to higher fluorescence values than those of control cells in a time-dependent manner. (d to e) Fluorescence histograms of control (black line) and CNF1-treated (gray line) cells stained with FITC-DNase I, which labels monomeric actin. No difference was detected between control and treated cells. (g to i) Fluorescence histograms of control (black line) and CNF1-treated (gray line) cells stained with anti-actin antibodies. After 24 h of treatment, an increase in total actin expression was detectable. (l to n) Volume histograms of overlying control (●) and CNF1-treated (▲) cells. Cell measurements are distributed on 225 channels from 0,656E3 to 5,420E3 fl.

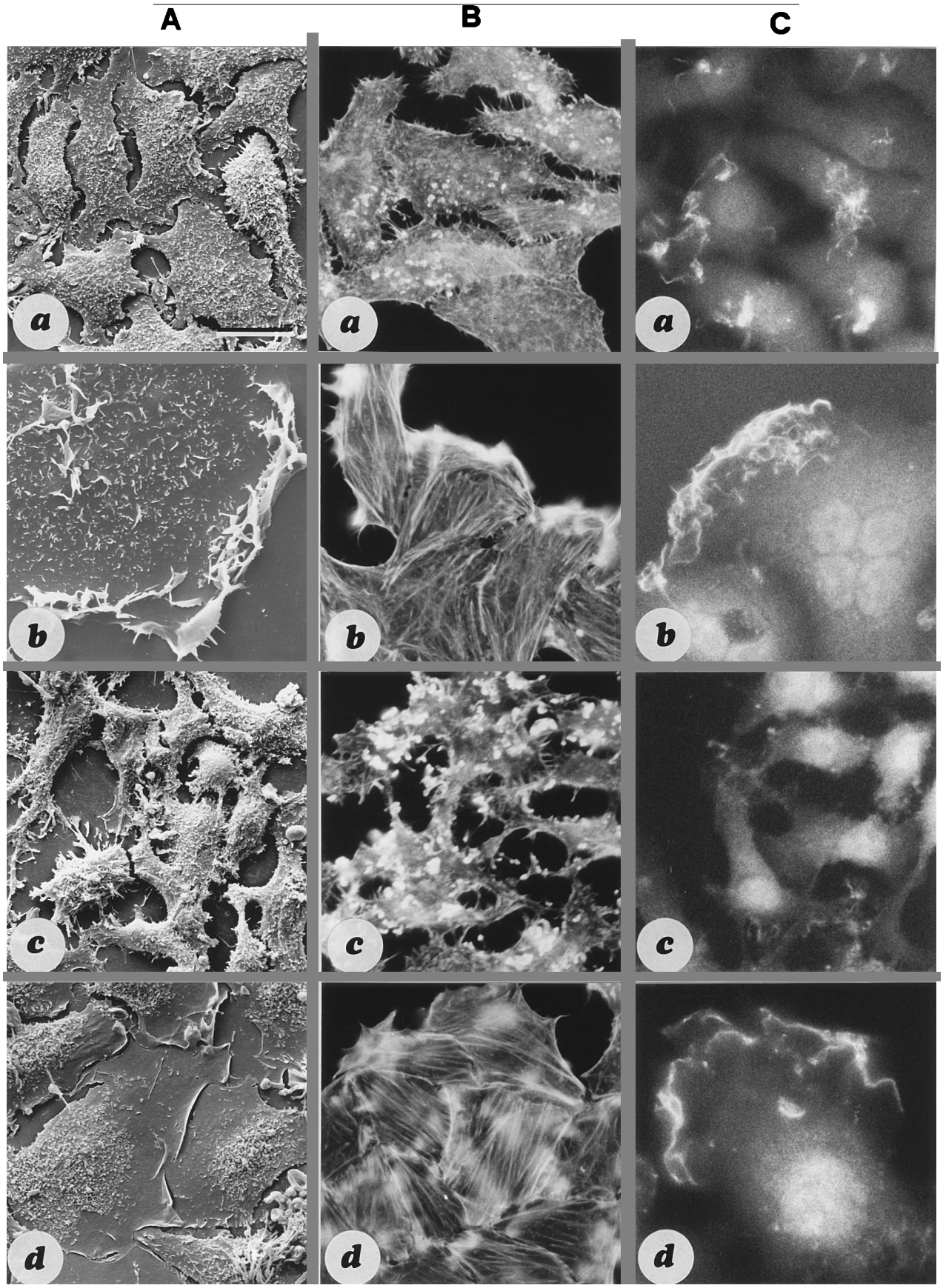

FIG. 2. CNF1 overcomes the inactivation of Rho by *C. botulinum* exoenzyme C3 in HEp-2 cells. (A) Scanning electron micrographs of control cells (a), cells exposed to CNF1 for 48 h (b), cells exposed to C3B for 36 h (c), and cells treated simultaneously with CNF1 and C3B (d); (B) fluorescence micrographs of cells stained for F-actin detection and treated with toxins as described for panel A; (C) fluorescence micrographs of cells stained for fimbrin localization and exposed to toxins as described for panel A. Cells treated simultaneously with the two toxins showed the same phenotype as CNF1-treated cells.

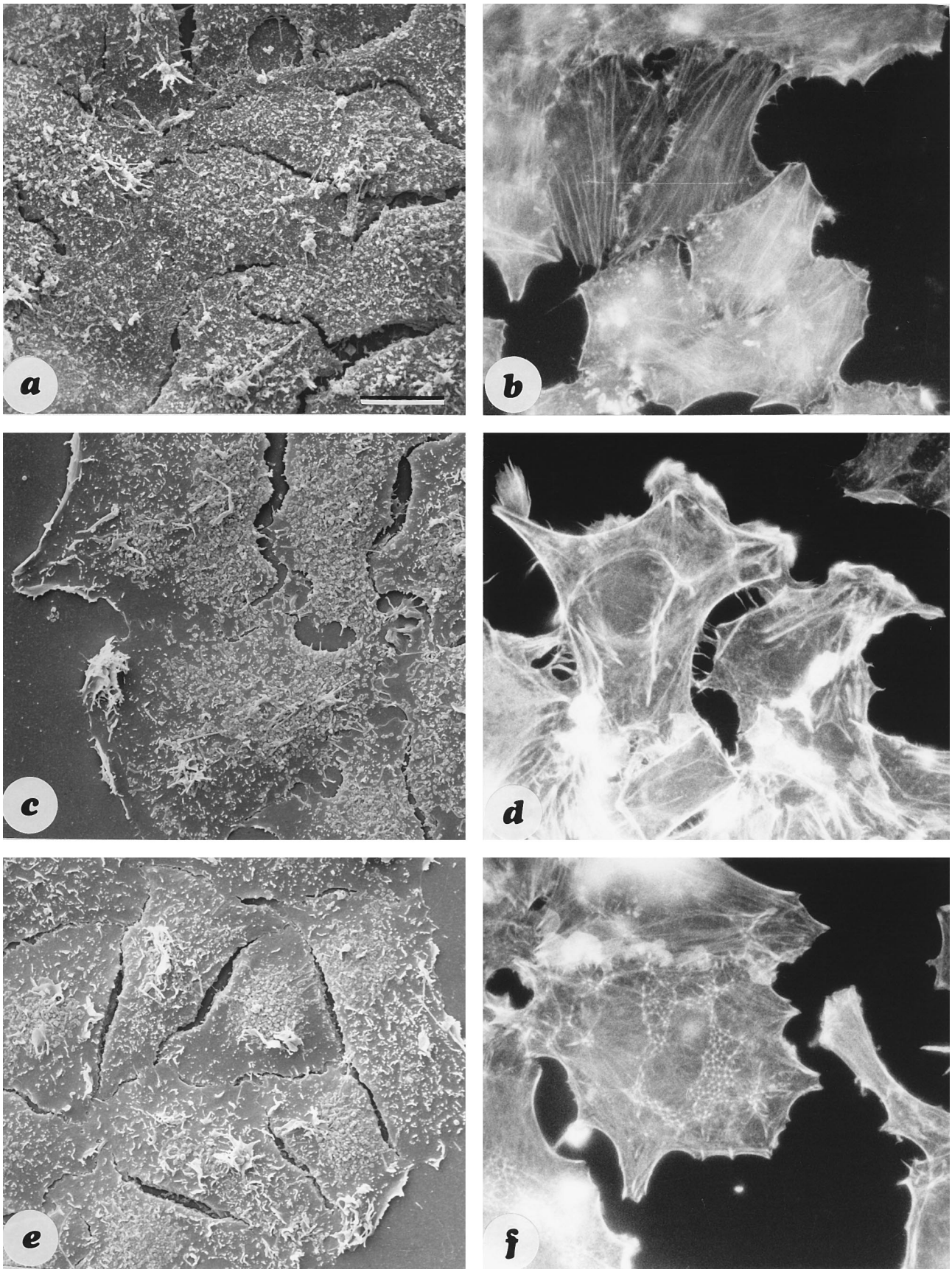

FIG. 3. Scanning (left panels) and fluorescence (right panels) micrographs of HEp-2 cells. (a to d) After exposure to C3B for 36 h, cells were treated with CNF1 for 6 (a and b) and 48 (c and d) h. Already after 6 h of CNF1 treatment, the C3 phenotype was almost completely reverted, in terms of both surface morphology and microfilament organization. (e and f) Cells were pretreated with CNF1 for 48 h before the addition of C3B. This clearly prevented the cell retraction induced by C3B.

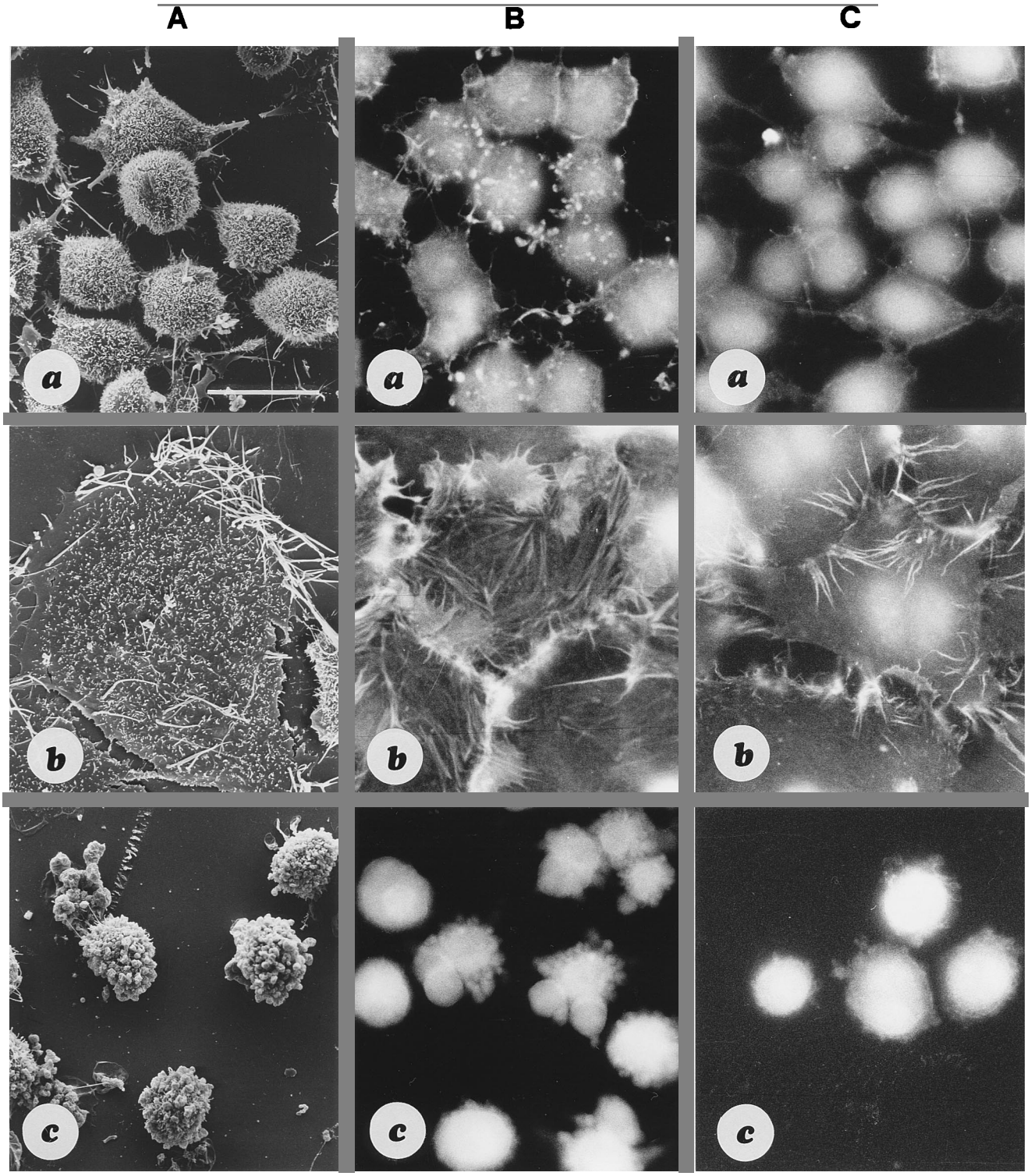

FIG. 4. CNF1-treated HEp-2 cells are resistant to CdB. (A) Scanning electron micrographs of cells exposed to CdB for 4 h (a), cells treated first with CNF1 and then with CdB (b), and cells pretreated with CdB and then exposed to CNF1 (c); (B) fluorescence micrographs of cells stained for F-actin detection and treated with toxins as described for panel A; (C) fluorescence micrographs showing the fimbrin distribution in cells exposed to toxins as described for panel A. In the latter two cases, the cells were insensitive to the second toxin added.

48 h induced a total disappearance of the C3B phenotype (Fig. 3c and d). Incubation of HEp-2 cells with CNF1 for 48 h followed by treatment with C3B for 36 h did not change the CNF1 phenotype of the cells (Fig. 3e and f).

CNF1-treated HEp-2 cells are resistant to CdB. CdB modifies posttranslationally the Rho molecule by a new type of reaction and inactivates this GTP-binding protein (20), triggering the disruption of the microfilament system in cells. CdB

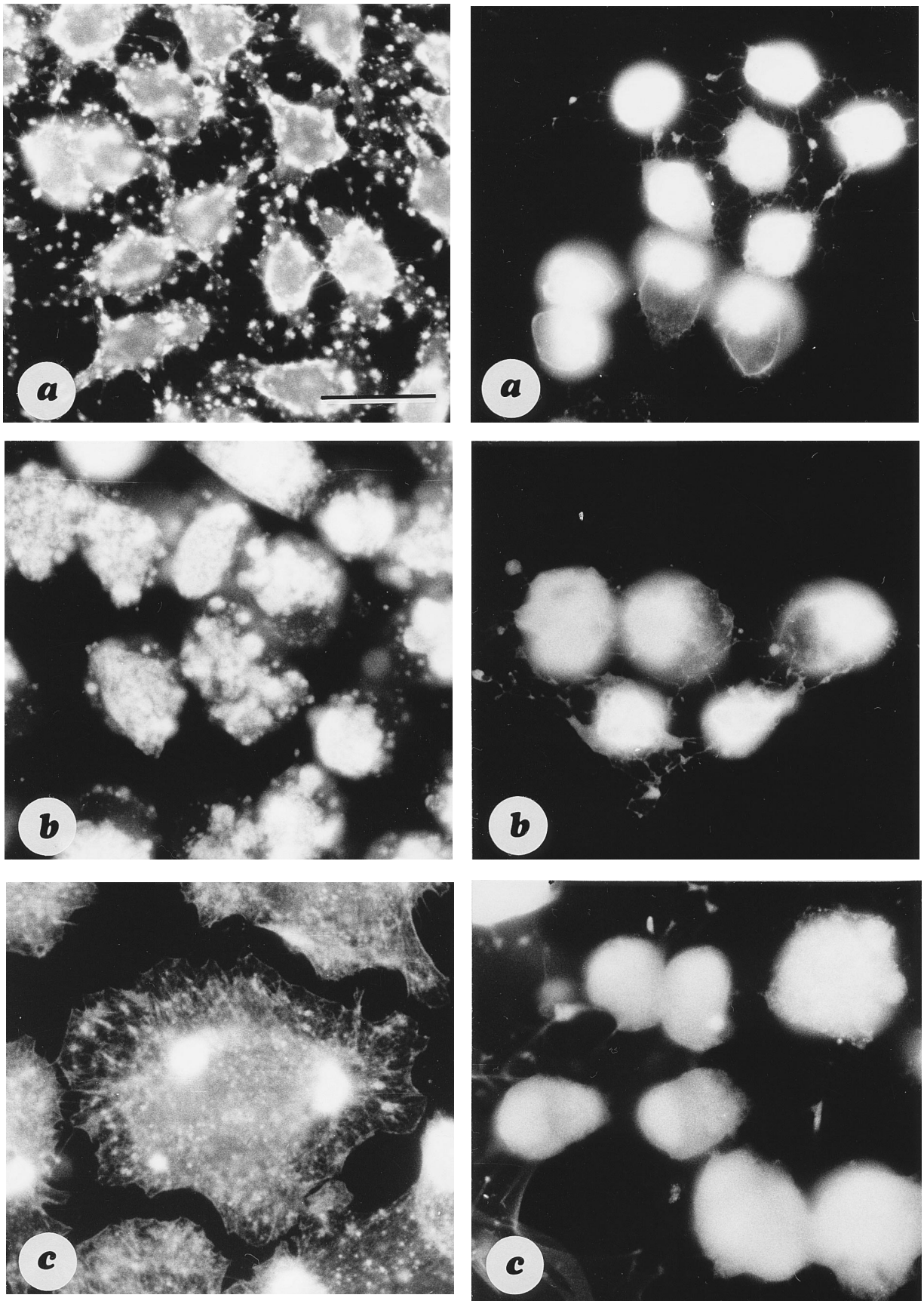
A
B
a
a
b
b
c
c

was used to probe CNF1 activity on Rho in cells. As observed by scanning electron microscopy (Fig. 4A), cells treated with CdB for 4 h showed an evident cell retraction and rounding (Fig. 4Aa). These phenomena were prevented by cell preincubation with CNF1 for 48 h, before exposure to CdB (Fig. 4Ab). Conversely, when HEp-2 cells were first treated with CdB and then incubated with CNF1, they maintained the CdB-induced phenotype (Fig. 4Ac). By use of fluorescence microscopy, a complete disorganization of the cell actin meshwork was observed after 4 h of treatment with CdB alone (Fig. 4Ba) as well as when CdB-treated cells were further incubated with CNF1 (even as long as 48 h) (Fig. 4Bc). Preincubation of HEp-2 cells with CNF1 for 48 h prevented CdB-induced changes in F-actin organization (Fig. 4Bb). In these conditions, F-actin structures appeared to be organized mainly as they were in CNF1-treated cells (Fig. 4Bb). Fimbrin distribution was also modified following HEp-2 cell treatment with CdB (Fig. 4C). Complete disappearance of fluorescent staining for fimbrin was observed after CdB exposure (Fig. 4Ca). Preincubation with CNF1 prevented the modification induced by CdB alone (Fig. 4Cb). Finally, exposure of the cells first to CdB and then to CNF1 induced a total disappearance of fimbrin staining as observed in cells treated with CdB alone (Fig. 4Cc). The blebbing phenomenon observed in cells treated first with CdB and then with CNF1 for 48 h is most probably due to the long exposure of cells to CdB.

CNF1 does not impair toxins which depolymerize microfilaments in a Rho-independent fashion. CD (10) and *C. spiroforme* iota-like toxin (3, 26) depolymerize microfilaments by binding or directly modifying actin. We thus used these agents to control the action of CNF1 on HEp-2 cell F-actin structures. By use of fluorescence microscopy, complete disorganization of the cell actin meshwork was observed after 4 h of treatment with CD (Fig. 5Aa). Although the fluorescence pattern of F-actin obtained after 18 h of incubation of cells with *C. spiroforme* was different from the one observed with CD, it is evident that also in this case, all actin structures were totally disrupted (Fig. 5Ba). Complete disorganization of microfilaments was still detectable after exposure of cells to CD for 4 h and then to CNF1 for 48 h (Fig. 5Ab). Pretreatment with CNF1 for 48 h did not protect cells against actin depolymerization induced by CD (Fig. 5Ac). HEp-2 cells preincubated with CNF1 and then challenged with iota-like toxin exhibited an iota-like F-actin phenotype (Fig. 5Bb). The same effect was observed when HEp-2 cells were first incubated with iota-like toxin and then treated with CNF1 for 48 h (Fig. 5Bc).

DISCUSSION

In this article, we have shown that exposure of HEp-2 cells to CNF1 induced reorganization of G-actin into F-actin, probably through activation of the Rho GTPase. Treatment with CNF1 rendered HEp-2 cells resistant to the F-actin disrupting effects of either CdB or *C. botulinum* exoenzyme C3, both known to act on the Rho GTPase (9, 20). The activity of CNF1 on Rho appeared to be specific, since agents or toxins which disturb actin polymerization in a Rho-independent fashion had no effect on microfilaments in cells pretreated with CNF1. Along with the recent demonstration that in CNF1-treated cells the Rho protein was probably covalently modified (17, 23), these results suggest that CNF1-induced actin polymerization may be due to constitutive activation of the Rho GTPase.

In cells, polymerization of G-actin into F-actin was not detectable by fluorescence-activated cell sorter (FACS) analysis before 24 h of CNF1 treatment. After 24 h, the increase of F-actin induced by CNF1 was detected without a concomitant decrease in the G-actin cytosolic pool. These results suggest that at the onset of its activity on cells, CNF1 induced actin polymerization in only a small part of the total G-actin cell content not detectable by FACS. This observation therefore suggests that CNF1 activates a regulatory protein such as Rho involved in actin polymerization at the level of specific structures like focal adhesion points. The increase in F-actin found in cells after 24 h of CNF1 treatment may account for activation of a large amount of the Rho protein. It is interesting that together with the detected increase in F-actin content, the CNF1-treated cell volumes were also considerably augmented. Increase in cell volume may be due to impairment of cytokinesis, as reported previously (16), but probably also to the spreading of cells induced by CNF1. Cell spreading requires F-actin structures (21), and therefore the increase in F-actin content of CNF1-treated cells may be involved in this function.

Pretreatment of HEp-2 cells with CNF1 rendered them resistant to *C. botulinum* exoenzyme C3. This enzyme is known to ADP-ribosylate the Rho GTPase on asparagine 41 (29). Rho asparagine 41 is in the vicinity of the effector region of the GTPase. It was therefore postulated that upon ADP-ribosylation, the Rho molecule can no longer interact with its effector. Resistance of CNF1-treated cells to exoenzyme C3 can be explained by the fact that Rho in these cells has became a dominant positive regulator, thus constitutively bound to its effector molecule. Being bound to its effector, the Rho GTPase, in CNF1-treated cells, cannot be ADP-ribosylated by exoenzyme C3. This will result in C3B being unable to convert the CNF1 to the C3 cell phenotype. Our observation that cells treated first with C3B and then with CNF1 showed a CNF1 phenotype can be explained by the existence of a pool of the Rho GTPase having an extremely low ability to be ADP-ribosylated by C3 but which can react with CNF1. In fact, it has been shown that Rho complexed to its guanine dissociation inhibitor (30) has a lower capacity to be ADP-ribosylated by C3 than Rho alone. Since most of the Rho protein in cells is in soluble form complexed to guanine dissociation inhibitor, exoenzyme C3 modifies in vivo mainly that fraction of the GTPase free from guanine dissociation inhibitor. Upon CNF1 treatment, the pool of Rho not ADP-ribosylated by C3 could be modified by CNF1 and thus activated by this factor.

CdB is also a bacterial protein whose intracellular target is the Rho GTPase (20). Most of CdB activities on the actin cytoskeleton can be explained by modification of the Rho GTPase into a dominant negative inhibitor. We have shown that pretreatment of HEp-2 cells with CNF1 for 48 h made them resistant to the challenge by CdB. In CNF1-treated cells, if Rho behaves as a dominant activator (permanently linked to its effector molecule), the GTPase might be protected against CdB-induced modification. However, CdB-treated cells were not sensitive to CNF1, since the phenotype induced by CdB could not be reversed by CNF1. Therefore, the covalent modification induced on Rho by CdB is probably, by contrast to

FIG. 5. Fluorescence micrographs of HEp-2 cells stained for F-actin detection. (Aa) Cells treated with CD for 4 h; (Ab) cells exposed first to CD for 4 h and then to CNF1 for 48 h; (Ac) cells pretreated with CNF1 before the addition of CD. (Ba) Cells exposed to *C. spiroforme* iota-like toxin for 18 h; (Bb) cells pretreated with iota-like toxin and then exposed to CNF1; (Bc) cells treated first with CNF1 and then with iota-like toxin. CD and iota-like toxin interfere with the actin assembly induced by CNF1.

exoenzyme C3, extremely efficient, reaching most if not all of the Rho molecules of the cell.

One of the most striking features observed in CNF1-treated cells is the formation of ruffles. In these F-actin structures, thick microfilaments cross-linked to the actin-binding and -bundling fimbrin were clearly noticed. It has been shown that ruffles are extremely dynamic F-actin structures which are made of short F-actin segments (each of about 200 actin monomers) rapidly cross-linked with actin-bundling proteins such as fimbrin. We can thus infer that in CNF1-treated cells, F-actin structures are synthesized as short actin segments as a result of the activation of the Rho GTPase by this bacterial factor. It has been shown that both Rho and Rac control actin stress fibers in Swiss 3T3 cells, whereas Rac, but not Rho, also regulates membrane ruffling (28). On the other hand, Rho has been reported to be involved in hepatocyte growth factor- and phorbol ester-induced membrane rufflings in KB cells (22). Interestingly, this Rho-dependent ruffling is very similar to the ruffling promoted by CNF1 in HEp-2 cells.

Finally, the specific activity of CNF1 on the Rho GTPase was highlighted by the observation that CNF1 did not protect cells treated with either CD or *C. spiroforme* iota-like toxin. Indeed, we have shown that pretreatment of cells with CNF1 followed by a challenge with CD or *C. spiroforme* toxin did not modify the phenotype induced by these agents. Also, incubation of cells with CNF1 after exposure to CD or *C. spiroforme* iota-like toxin could not revert the cell phenotype induced by these actin-modifying drugs.

All of our results therefore point out that CNF1 modifies the Rho GTPase in such a way as to induce a dominant positive activity of these GTP-binding proteins. This will achieve a stable association of the Rho proteins with their putative effector(s) molecule(s), leading to the protection of the GTPases against other toxins able to modify Rho. Thus, CNF1-treated cells could represent a useful experimental system to isolate a molecule(s) involved in the Rho regulatory cascade.

ACKNOWLEDGMENT

This work was partially supported by National Research Council Targeted Project "Prevention and Control of Disease Factors," subproject 3, grant 94.00685.PF41, to G. Donelli.

REFERENCES

1. **Abo, A., E. Pick, A. Hall, N. Totty, C. G. Teahan, and A. W. Segal.** 1991. Activation of the NADPH oxidase involves the small GTP-binding protein p21rac1. Nature (London) **353:**668–670.
2. **Aktories, K., S. Rosener, U. Blaschke, and G. S. Chhatwal.** 1988. Botulinum ADP-ribosyltransferase C3. Eur. J. Biochem. **172:**445–450.
3. **Aktories, K., and A. Wegner.** 1989. ADP-ribosylation of actin by clostridial toxins. J. Cell Biol. **109:**1385–1387.
4. **Aullo, P., M. Giry, M. R. Popoff, C. Kocks, and P. Boquet.** 1993. A chimeric toxin to study the role of the 21 kDa GTP binding protein rho in the control of actin microfilament assembly. EMBO J. **12:**921–931.
5. **Blanco, J., M. P. Alonso, E. A. Gonzalez, M. Blanco, and J. I. Garabal.** 1990. Virulence factors of bacteraemic *Escherichia coli* with particular reference to production of cytotoxic necrotising factor (CNF) by P-fimbriate strains. J. Med. Microbiol. **31:**175–183.
6. **Bretscher, A.** 1981. Fimbrin is a cytoskeletal protein that crosslinks F-actin *in vitro*. Proc. Natl. Acad. Sci. USA **78:**6849–6853.
7. **Caprioli, A., V. Falbo, L. G. Roda, F. M. Ruggeri, and C. Zona.** 1983. Partial purification and characterization of an *Escherichia coli* toxic factor that induces morphological cell alterations. Infect. Immun. **39:**1300–1306.
8. **Caprioli, A., V. Falbo, F. M. Ruggeri, L. Baldassarri, R. Bisicchia, G. Ippolito, E. Romoli, and G. Donelli.** 1987. Cytotoxic necrotizing factor production by hemolytic strains of *Escherichia coli* causing extraintestinal infections. J. Clin. Microbiol. **25:**146–149.
9. **Chardin, P., P. Boquet, P. Madaule, M. R. Popoff, E. J. Rubin, and D. M. Gill.** 1989. The mammalian G protein Rho C is ADP-ribosylated by *Clostridium botulinum* exoenzyme C3 and affects actin microfilaments in Vero cells. EMBO J. **8:**1087–1092.
10. **Cooper, J. A.** 1987. Effects of cytochalasin and phalloidin on cells. J. Cell Biol. **105:**1473–1478.
11. **Donelli, G., C. Fiorentini, L. Falzano, M. Pouchelet, E. Oswald, and P. Boquet.** 1994. Effects induced by cytotoxic necrotizing factor 1 (CNF1) from pathogenic *E. coli* on cultured epithelial cells. Zentralbl. Bakteriol. Suppl. **24:**60–71.
12. **Falbo, V., M. Famiglietti, and A. Caprioli.** 1992. Gene block encoding production of cytotoxic necrotizing factor 1 and hemolysin in *Escherichia coli* isolates from extraintestinal infections. Infect. Immun. **60:**2182–2187.
13. **Falbo, V., T. Pace, L. Picci, E. Pizzi, and A. Caprioli.** 1993. Isolation and nucleotide sequence of the gene encoding cytotoxic necrotizing factor 1 of *Escherichia coli*. Infect. Immun. **61:**4909–4914.
14. **Falkow, S., R. Isberg, and D. A. Portnoy.** 1992. The interaction of bacteria with mammalian cells. Annu. Rev. Cell Biol. **8:**333–363.
15. **Falzano, L., C. Fiorentini, G. Donelli, E. Michel, C. Kocks, P. Cossart, L. Cabanié, E. Oswald, and P. Boquet.** 1993. Induction of phagocytic behaviour in human epithelial cells by *Escherichia coli* cytotoxic necrotizing factor type 1. Mol. Microbiol. **9:**1247–1254.
16. **Fiorentini, C., G. Arancia, A. Caprioli, V. Falbo, F. M. Ruggeri, and G. Donelli.** 1988. Cytoskeletal changes induced in HEp-2 cells by the cytotoxic necrotizing factor of *Escherichia coli*. Toxicon **26:**1047–1056.
17. **Fiorentini, C., M. Giry, G. Donelli, L. Falzano, P. Aullo, and P. Boquet.** 1994. *E. coli* cytotoxic necrotizing factor 1 increases actin assembly via the p21 Rho protein. Zentralbl. Bakteriol. Suppl. **24:**404–405.
18. **Francis, C. L., T. A. Ryan, B. D. Jones, S. J. Smith, and S. Falkov.** 1993. Ruffles induced by salmonella and other stimuli direct macropinocytosis of bacteria. Nature (London) **364:**639–642.
19. **Hall, A.** 1994. Small GTP-binding proteins and the regulation of the actin cytoskeleton. Annu. Rev. Cell Biol. **10:**31–54.
20. **Just, I., G. Fritz, K. Aktories, M. Giry, M. R. Popoff, P. Boquet, S. Hegenbarth, and C. von Eichel-Streiber.** 1994. *Clostridium difficile* toxin B acts on the GTP-binding protein Rho. J. Biol. Chem. **269:**10706–10712.
21. **Lazarides, E.** 1976. Two general classes of cytoplasmic actin filaments in tissue culture cells: the role of tropomyosin. J. Supramol. Struct. **5:**531–537.
22. **Nishiyama, T., T. Sasaki, K. Takaishi, M. Kato, H. Yaku, K. Araki, Y. Matsuura, and Y. Takai.** 1994. rac p21 is involved in insulin-induced membrane ruffling and rho p21 is involved in hepatocyte growth factor- and 12-*O*-tetradecanoylphorbol-13 acetate (TPA)-induced membrane ruffling in KB cells. Mol. Cell Biol. **14:**2447–2456.
23. **Oswald, E., M. Sugai, A. Labigne, H. C. Wu, C. Fiorentini, P. Boquet, and A. D. O'Brien.** 1994. Cytotoxic necrotizing factor type 2 produced by virulent *Escherichia coli* shares sequence homology with *Pasteurella multocida* toxin and modifies a small GTP-binding protein involved in stress fiber formation in eukaryotic cells. Proc. Natl. Acad. Sci. USA **91:**3814–3818.
24. **Paterson, H. F., A. J. Self, M. D. Garret, I. Just, K. Aktories, and A. Hall.** 1990. Microinjection of recombinant p-21^{rho} induces rapid changes in cell morphology. J. Cell Biol. **111:**1001–1007.
25. **Popoff, M. R., and P. Boquet.** 1988. *Clostridium spiroforme* toxin is a binary toxin which ADP-ribosylates cellular actin. Biochem. Biophys. Res. Commun. **152:**1361–1368.
26. **Popoff, M. R., F. W. Milward, B. Bancillon, and P. Boquet.** 1989. Purification of the *Clostridium spiroforme* binary toxin and activity of the toxin on HEp-2 cells. Infect. Immun. **57:**2462–2469.
27. **Ridley, A. J., and A. Hall.** 1992. The small GTP-binding protein rho regulates the assembly of focal adhesions and actin stress fibers in response to growth factors. Cell **70:**389–399.
28. **Ridley, A. J., H. F. Paterson, C. L. Johnston, D. Diekmann, and A. Hall.** 1992. The small GTP-binding protein rac regulates growth factor-induced membrane ruffling. Cell **70:**401–410.
29. **Sekine, A., M. Fujwara, and S. Narumiya.** 1989. Asparagine residue in the rho gene product is the modification site for botulinum ADP-ribosyltransferase. J. Biol. Chem. **264:**8602–8605.
30. **Takai, Y., K. Kaibuchi, A. Kikuchi, and M. Kawata.** 1992. Small GTP-binding proteins. Int. Rev. Cytol. **133:**187–229.